Notch strength insensitivity of self-setting hydroxyapatite bone cements

JANE P. MORGAN, REINHOLD H. DAUSKARDT*
Department of Materials Science and Engineering, Stanford University, Stanford, CA 94305, USA
E-mail: dauskardt@stanford.edu

The effect of notches on the strength properties of self-setting hydroxyapatite (HA) cements is examined. Such stress concentrators may be present at orthopedic repair sites employing cements and significantly affect their mechanical reliability. Notched tensile specimens were prepared from two cement compositions that resulted in HA and carbonated apatite. The notch radii was varied from 0.15 to 6 mm with a fixed length of 6 mm. The strength of the cements was found to be surprisingly insensitive to the presence of the notches over the range of notch radii examined. A fracture statistics model incorporating a Weibull statistical approach was employed to rationalize the observed notch insensitivity.

1. Introduction

Self-setting hydroxyapatite [$Ca_{10}(PO_4)_6(OH)_2$] (HA) bone cements have received significant attention since the 1980s due to their similarity to the natural phase of bone [1]. When mixed at physiological conditions with sodium phosphate solution, these cements form HA as the only end product [2]. Despite their favorable biocompatible properties, the brittle nature of HA cements yields inferior strengths when compared to natural bone [3–6]. The increased use of HA cements in a range of orthopedic applications provides compelling motivation for an improved understanding of the underlying microstructural mechanisms that govern the useful strength of these materials. In particular, in this study, we explored the effects of notch radius on the tensile fracture strength of two HA cement formulations.

From a strength-of-materials standpoint, analyzing how a brittle material behaves in the presence of a stress concentrator like a notch is integral to understanding the mechanical reliability of the material. From a clinical standpoint, it is of considerable importance to understand the effects of notches or stress concentrators that might be present at orthopedic repair sites. These might involve protrusions of hard or soft tissue into the bone cement, large air or fluid pockets, or even geometrically sharp features associated with prosthetic devices or fixtures. Notch sensitive materials typically exhibit significantly reduced strength in the presence of such stress concentrators and may fail prematurely. Surprisingly, however, to the authors knowledge, there are currently no reported studies of the notch sensitivity of self-setting HA bone cements.

The effect of machined notches has been reported for mature bovine Haversian bone by Lakes *et al*. [7]. They performed notched tensile experiments on bovine Haversian bone and found that the tensile fracture strength was reduced. However, the notched tensile fracture strength was higher in the presence of a notch than that predicted using a conventional maximum stress approach. In this approach, the strength of the notched material is predicted by setting the maximum stress at the notch tip equal to the inherent strength of the material. They concluded that Haversian bovine bone resists small stress concentrations like fatigue micro-cracks and saw cuts to a much greater extent than predicted by the maximum notch stress. The immunity to stress concentrations was rationalized in terms of a strain redistribution of the Haversian bone architecture that was approximated using Cosserat elasticity [7].

In the present study, the primary interest was to determine whether HA cements are stronger in the presence of stress concentrations than expected based on their previously reported mechanical properties [6, 8]. The two commercial cement formulations examined resulted in final compositions of either precipitated HA or carbonated apatite. Tensile notch specimens were prepared with machined notch radii ranging from 0.15 to 6 mm. The notch tensile strengths of the HA cements were found to be surprisingly insensitive to notch radius. With a change of over an order of magnitude in notch radius there was virtually no change in tensile fracture strength. The lack of notch sensitivity was attributed to the mutually competing effects of the local notch maximum stress and the notch area actually exposed to the increased stress. Decreasing the notch radius increases the notch stress but also reduces the probability of there being a strength controlling flaw on the notch surface. A weakest link fracture statistics model using

*Author to whom all correspondence should be addressed.

Weibull statistics and modified to account for the presence of the notch was employed to predict the observed notch insensitivity of the two HA cements.

2. Experimental procedure

Specimens were prepared from two commercially available HA cements. The CaP cement (Bone Source™, Stryker Howmedica Osteonics, Rutherford, NJ) had a powder formulation containing tetracalcium phosphate and dicalcium phosphate. The CaP/CO_3 cement had a powder formulation containing tricalcium phosphate, calcium carbonate and monocalcium phosphate monohydrate (Norian SRS™, Norian Corporation, Cupertino, CA). A sodium phosphate dibasic solution [0.075M $Na_2HPO_4 + H_2O$] was added to both powders at a liquid-to-solid ratio of 0.3 and 0.48 for the CaP and the CaP/CO_3 cements, respectively, according to the manufacturers recommendations. After addition of the sodium phosphate solution, a cementitious reaction involving an acid-base neutralization, dissolution/reprecipitation process commenced to form the final HA product. The mixture maintained a malleable consistency for approximately four to five minutes.

Rectangular specimens were made in a delrin mold from which two notch tensile specimens could be machined. The cement mixture was packed into the mold and was placed in a bath of phosphate buffered saline (PBS) solution at 37 °C for 1 h. The specimens were carefully removed from the mold and cured in PBS for more than 48 h prior to final specimen machining. After curing for 24 h, the cements have been reported to have a structure and composition similar to HA [$Ca_5(PO_4)_3OH$] with no significant further changes with curing time [3]. When fully cured, the block was cut using a diamond wafer saw into two specimens of length 50 mm, width 16 mm, and thickness 8 mm (Fig. 1). The notches with radii of 0.64–6 mm were machined on one side face of the specimen using milling tools. For the specimens with notches of radius 0.15 mm, a hand held wire saw with diamond wire was used to cut the notch. All notches were 6 mm in length.

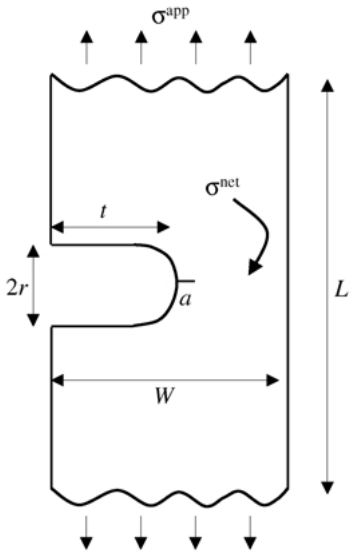

Figure 1 Notched bar specimen geometry indicating the notch radius, *r*, the notch length, *t*, the width of the specimen, *W*, the length, *L*, and the crack length ahead of the notch tip, *a*. *r* varied from 0.15–6 mm. *t* was constant at 6 mm.

Aluminum loading tabs were affixed to each specimen using a waterproof epoxy in a mounting device that assured the tabs were aligned accurately. The epoxy was cured dry at room temperature for 12 h prior to testing. All tests were performed with the specimens mounted vertically in tension on a screw driven mechanical testing machine (MTS Bionix 200 with a 1 kN load cell, MTS Corporation, Eden Prairie, MN) at a displacement rate of 0.7 μm/s. The loads and displacements were continuously recorded during testing and the notch tensile strength, σ_f^{net}, was determined from the maximum applied load and the net section area of the specimen ahead of the notch tip. The displacements were measured on the load frame and the compliance of the frame was subtracted when calculating the engineering strain imposed on the specimen.

In order to determine the inherent strength of the CaP cement, rectangular specimens were made with the same delrin mold and tested in four-point bending to determine the average strength and Weibull modulus similar to previously reported studies of the CaP/CO_3 cement [9]. The blocks were cut into four specimens using the diamond wafering saw. They were removed from the PBS bath after a 48 h cure and sanded using 600 grit SiC paper. Testing was conducted wet on an electro-servo-hydraulic mechanical test system (MTS 810 load frame 458.20 controller, MTS Corporation). Specimens were loaded using a fully articulating four point bending fixture in displacement control at a displacement rate of 0.7 μm/s. Load and displacement data was continuously recorded. The ultimate load prior to specimen fracture was used to determine the maximum flexural strength and reported using a Weibull failure probability plot similar to previous studies of the CaP/CO_3 cement [9].

The fracture surfaces of the notched specimens were examined using a scanning electron microscope (SEM). The surfaces were sputtered for 200 s with gold to reduce charging prior to examination in the SEM.

3. Results

A representative net section stress versus applied strain plot for a CaP specimen with a notch radius of 2.45 mm is shown in Fig. 2. At low stresses, the deviation from linearity apparent in the figure was due to removal of slack in the load train. At higher loads, linear elastic behavior was observed with no appreciable non-linearity indicative of plastic strain prior to fracture. All specimens failed in less than four minutes of loading, precluding the effects of any time-dependent subcritical crack-growth processes that have recently been observed in such materials [10]. The resulting net section notch strength, σ_f^{net}, of the specimen was taken as the maximum net section stress immediately prior to fracture and is shown as a function of notch radius in Fig. 3 for both cements. Also included in the figure is the total applied stress at fracture, σ_f^{app}, calculated from the full area of the specimen which will be used in the subsequent analysis. The data points represent the average notch strength of at least four specimens at

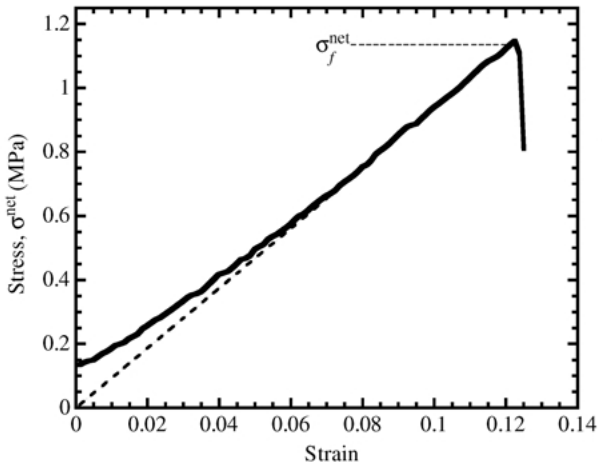

Figure 2 Net section stress versus applied strain plot for a 1.23 mm radius CaP cement sample. The deviation from linearity at low loads was due to taking-up of slack in the load train. The behavior is representative of the other CaP and CaP/CO_3 specimens with no plastic deformation evident preceding failure.

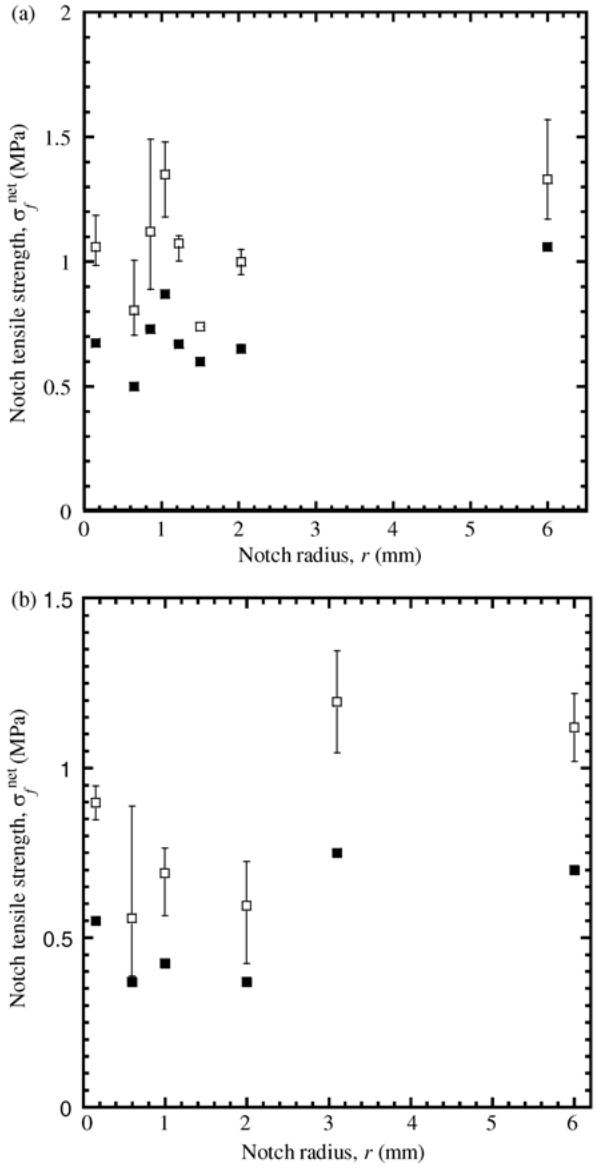

Figure 3 Notch tensile strength, σ_f^{net} vs. notch radius, r, data for (a) the CaP cement, and (b) the CaP/CO_3 cement. The open data points represent the average notch fracture strength, σ_f^{net}, of at least four specimens. The error bars indicate the maximum and minimum values observed. Included in the figure for comparison (closed data points) are the values for σ_f^{app} for both cements.

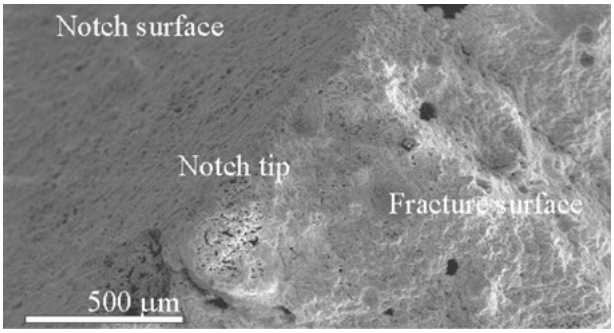

Figure 4 SEM micrograph of the notch tip region of a 2.45 mm radius CaP specimen. The left side shows the machined notch surface. The ridge in the middle of the micrograph is the notch tip and the fracture surface is on the right. Note the dark pores at the tip and along the fracture path. These pores are crack initiation sites and determine the strength of the material.

each radius. The error bars represent the maximum and minimum strength values obtained. Only specimens that failed at the notch are reported. Remarkably, no systematic variation of notch strength was observed for notch radii that varied from 0.15 to 6 mm. The average tensile notch strengths for the CaP and the CaP/CO_3 cements, σ_f^{net}, were 1.04 and 0.79 MPa, respectively. Typical of brittle materials, considerable scatter was apparent for strength values measured for each notch radius, and a similar scatter of average notch strength values was noted when comparing the different notch radii. However, the average notch strength for the CaP cement was statistically significantly higher than that of the CaP/CO_3 cement.

Following strength testing of the notch specimens, the resulting fracture surfaces were examined in the SEM to determine the failure site. A representative micrograph showing fracture from the notch tip of a CaP specimen is shown in Fig. 4. It was not always possible to determine the exact initiation site using the SEM, however, the presence of potential initiation sites in the form of small pores and other defects on or near to the notch surface were apparent.

The results of the flexure strength measurements for the CaP cement are presented in the form of a Weibull failure probability versus flexure strength plot in Fig. 5. Also included in the figure for comparison are previously reported results for the CaP/CO_3 cement [9]. Both cements had a Weibull modulus of $m \sim 5.5$. The average flexure strengths, σ_s, of the CaP and CaP/CO_3 cements were 2.52 and 2.37 MPa, respectively. Similar to the notch strength, the CaP cement was on average stronger than the CaP/CO_3 cement. The time to failure for the flexure specimens was, like for the notched specimens, under four minutes.

4. Discussion

Brittle materials like porous HA cements have been shown to behave like brittle cellular solids with a fracture strength that is flaw dominated [6]. Linear elastic behavior is controlled by cell wall bending and stretching to the fracture strength. The flaw size dependent fracture strength generally curtails any plastic deformation caused by cell wall microcracking and rotation [11].

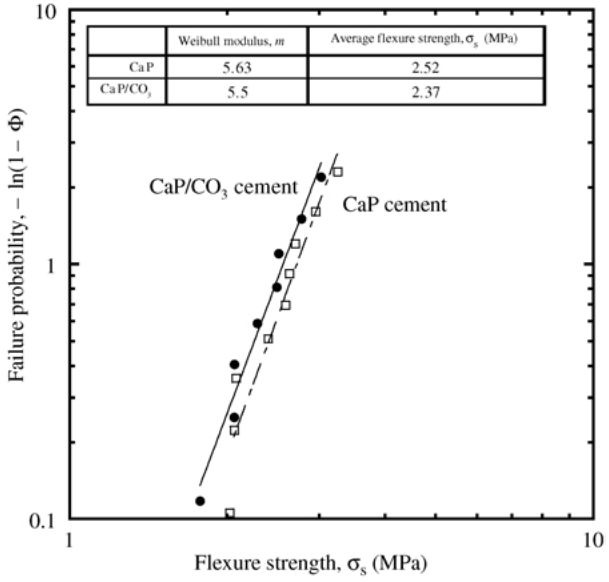

Figure 5 Weibull flexure strength plot for CaP and CaP/CO_3 cements. Strength data for the CaP/CO_3 cement is given for reference and was taken by Jew *et al*. [9].

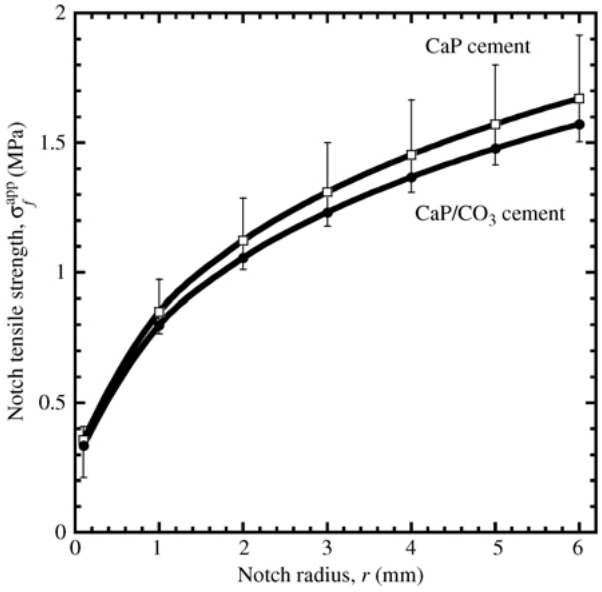

Figure 6 Predicted notch tensile strength values using the maximum stress criterion. The data points represent the expected notch tensile failure strength, σ_f^{app}, obtained from the average strength of the each cement, σ_s. The bars indicate the range of σ_f^{app} for a 90% failure probability and a 10% failure probability for the CaP cement. Similar behavior was apparent for the CaP/CO_3 cement. The model predicts a marked dependence of strength on notch radius.

The effect of a stress concentrator in the form of a notch on the strength of such brittle materials is often predicted by setting the maximum stresses at the tip of the notch equal to the fracture strength, σ_s, of the material. Modeling the notch as half an ellipse, and using the Inglis formula for an elliptical hole, the applied stress at fracture of the notched specimen, σ_f^{app}, is given by [12]:

$$\sigma_f^{app} = \frac{\sigma_s}{1 + 2(t/r)^{1/2}} Y \qquad (1)$$

where σ_s is the fracture strength of an unnotched specimen, t is the notch length, r is the notch radius of curvature, and $Y = 1.99$ is a geometric parameter that accounts for the finite width of the specimen [13]. Note here that σ_f^{app} is determined from the total cross sectional area of the specimen.

This simple model predicts that the applied stress at fracture should increase as a function of the square root of the notch radius, r, as shown in Fig. 6 for both cements. The data points represent the expected value of σ_f^{app} based on the average flexural fracture strength values, σ_s, of the cements reported in Fig. 5. The indicated scatter bands show the range of notch strengths expected for a 10% and 90% failure probability of the CaP cement obtained from the Weibull statistical analysis. A similar trend was apparent for the CaP/CO_3 cement. Notably, not withstanding the stochastic nature of flaw dominated strength values, this analysis predicts a marked dependence of strength on the specimen notch radius. Clearly, this was not the behavior observed experimentally.

The approach described above, however, neglects the phenomenon that for brittle materials where fracture strength is flaw dominated, the strength tends to decrease as the stressed area increases. The larger the surface area of the notched region, the greater the likelihood of finding a strength limiting flaw on the stressed surface. This effect competes with the effect of increasing notch radius and hence surface area which tends to lower the notch tip stresses as described by the simple model above.

In order to better understand these competing effects, a more complete model using a Weibull statistical approach that includes the notch surface flaw population was employed. The Weibull approach is a rank-order statistical method that is commonly used to describe the strength of brittle materials in terms of an inherent distribution of strength determining flaws [14]. The failure probability of notched ceramic bars in tension and bending has recently been treated using Weibull fracture statistics and forms the basis for the present analysis [15–17]. Details salient to the present analysis are summarized below. Geometrical parameters used are indicated in Fig. 1; specifically, r is the notch radius, t the notch length, and a is an assumed crack length emanating from the notch tip. Using this analysis, the two parameter failure probability can be written as [15]:

$$P = 1 - \exp\left(-\frac{S_{\text{eff}}}{S_0}\left(\frac{\sigma_s}{\sigma_0}\right)^m\right) \qquad (2)$$

where S_0 is a reference or unit surface, S_{eff} an effective surface, σ_s is the specific strength value corresponding to the failure probability P, and σ_0 and m the Weibull parameters.

The slope of a log–log plot of failure probability versus strength is the Weibull modulus, m, an indicator of the extent of the strength distribution. For example, steel has a deterministic strength with little scatter and a high Weibull modulus of ~ 100, while the strength of chalk is dependent on a wide distribution of flaw sizes and has a low Weibull modulus of ~ 5. The strength of the material is determined by the worst case flaw, specifically the flaw with the most adverse combination of size, stressed location and orientation. Considering only flaws orientated normal to the applied tensile stress, the

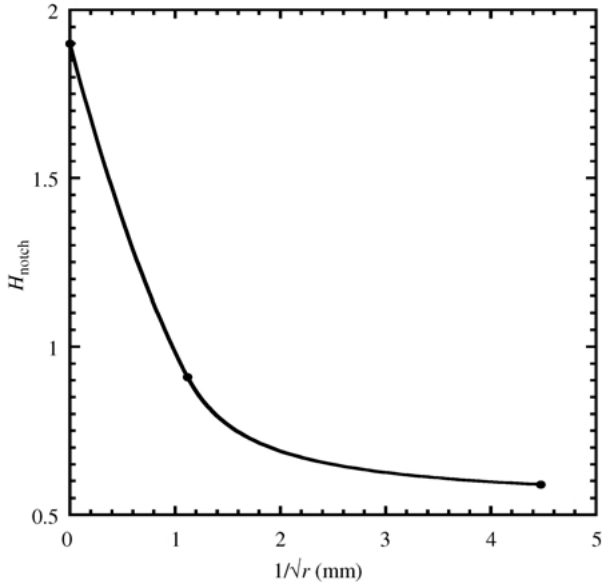

Figure 7 Plot of H_{notch} as a function of $1/\sqrt{r}$ for a material with a Weibull modulus of 5. Values of H_{notch} for this work were interpolated from the boundary element method calculations done by Hertel *et al*. [16].

resulting strength, σ_s, is related to the critical crack or flaw size, a_c, by the well-known fracture condition [18]:

$$\sigma_s = \frac{K_{lc}}{F\sqrt{a_c \pi}} \tag{3}$$

where K_{lc} is the fracture toughness of the cement, F a geometric parameter, and a_c the critical crack length. The plane strain fracture toughness has been measured for the CaP and the CaP/CO_3 cements and is 0.23 MPa$\sqrt{m}$ [8] and 0.14 MPa$\sqrt{m}$ [6], respectively. These values for K_{lc} are used in the following analysis.

The following normalized parameter, H, is introduced [16, 17]:

$$H = \left(\frac{S_{eff}}{S_0}\right)^{1/m} \tag{4}$$

which derives from the surface area or volume integrals in the Weibull analysis. This normalization provides a convenient method to compare the effect of different spatial stress distributions resulting from different geometries [15]. Using Equations 3 and 4, the failure probability as a function of flaw size at the notch tip can now be written as:

$$P(a) = 1 - \exp\left(-\left(H^2 \frac{a_0}{a_c}\right)^{m/2}\right) \tag{5}$$

where a_0 and a_c are the critical flaw lengths corresponding to σ_0 and σ_s, respectively. The utility of the normalized parameter, H, is apparent in the following expression which obtains from considering the same failure probability for planar and notched specimens [17]:

$$a_c^{notch} = a_c^{plane}\left(\frac{H_{notch}}{H_{plane}}\right)^2 = a_c^{plane}\left(\frac{S_{eff}^{notch}}{S_{eff}^{plane}}\right)^{1/m} \tag{6}$$

where the *notch* and *plane* subscripts and superscripts refer to values pertaining to a notched bar and a plane reference bar. The ratio H_{notch}/H_{plane} is a function of the Weibull modulus, m, and the notch radius, r. H_{notch}/H_{plane} increases with increasing Weibull modulus and notch radius to a value of 1. For large m, the strength is deterministic and equal to the maximum normal stress at the notch tip. Alternatively, notches with large radii do not concentrate stresses and act like planar surfaces. In both cases, $a_c^{notch} = a_c^{plane}$. For intermediate cases, the competing effects of the stress concentrating effect of the notch and the area exposed to the elevated notch stresses are reflected by a decreasing value of H_{notch}/H_{plane} with decreasing radius that is sensitive to the distribution of strength determining flaws.

The variation of H_{notch} with notch radius for the present cements with a Weibull modulus of ~ 5 was found by interpolation of the more general results obtained by numerical calculations previously reported [16]. Results are presented in Fig. 7. The results suggest that the equivalent critical defect size at the tip of a notch is smaller than that of a planar surface. What remains to be determined is the applied stresses needed to cause failure associated with the reduced defect size at the notch tip. This can readily be obtained by employing fracture mechanics solutions to obtain the stress intensity factor for the critical surface flaw ahead of the notch tip. The flaw ahead of the notch tip is assumed to be a through crack of length a_c^{notch} and the applied stress at fracture, σ_f^{app}, becomes [17]:

$$\sigma_f^{app} = \frac{K_{lc}}{\sqrt{\pi(a_c^{notch} + t)}F_{notch}\tanh\left(\gamma\sqrt{\frac{a_c^{notch}}{r}}\right)} \tag{7}$$

where γ is an analytical function that varies from 2.243 for notches with r/t approaching 0 to over 3 for very wide notches. For the present specimens, γ was only slightly dependent on notch radius and varied from 2.3 to 3.1 [17]. F_{notch} is a geometric function of specimen dimensions including the notch length, the specimen width and length. For a specimen with a side notch tested in tension, $F_{notch} = 3.625$ and is constant with increasing notch radius. The values for K_{lc} and t do not vary with notch radius. The solution to Equation 7 is appropriate for specimens where the notch radius, r, is less than half the notch length, t [19]. When the notch radius approaches zero, as is the case for a crack of atomic radius, Equation 7 reduces to Equation 3 as the hyperbolic tangent term goes to 1.

For the analysis, a_c^{plane} was found using Equation 3 and the values for σ_s determined experimentally (Fig. 5). $F = 1.12$ for a plane bar, and the values for K_{lc} for both cements are reported above. Subsequently, a_c^{notch} was determined at each notch radius using Equation 6 and the ratio of H_{notch}/H_{plane} from Fig. 7. The resulting predicted notch strength values, σ_f^{app}, from Equation 7 are presented in Fig. 8 as a function of notch radius for both cements. The model predicts the strength of notched specimens to be insensitive to notch radius over the range of notch radii examined.

The model predictions are clearly consistent with the observed insensitivity of the measured notch strength values to the notch radii (Fig. 3). Although the model under predicts the applied stress required to cause failure

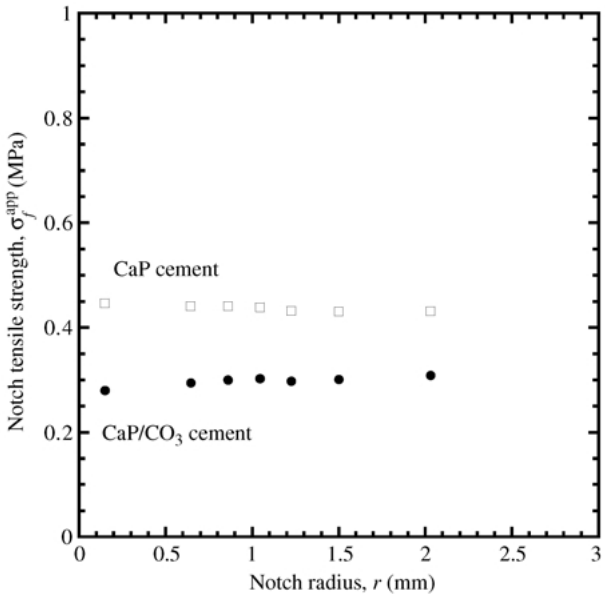

Figure 8 Notch tensile strength values, σ_f^{app}, as a function of the notch radius, r, predicted using the Weibull statistical model that incorporates the effect of the notch surface area and stress concentration.

of the notched bars, using only the fracture toughness and strength properties obtained from smooth flexure bars, it correctly predicts the insensitivity of the strength to the variation of the notch radius. This is a result of including both the effect of the notch on elevating the local notch stresses as well as on reducing the surface area and hence flaw population actually exposed to the elevated stresses. We note that the higher measured notch strengths compared to those predicted by the model may result from the surface finish of the notches, although no apparent difference in surface finish could be detected under close scrutiny in the SEM.

The effect of the extent of the strength-determining flaw size distribution, as determined by the value of the Weibull modulus, is important in rationalizing the present results. The effect of the Weibull modulus on the parameter H has been determined for a wide range of values [16]. The value of H_{notch} for all notch radii begins to approach H_{plane} when the Weibull exponent is greater than 20. This means that the critical flaw size for a notched specimen approaches the critical flaw size for a plane bar. For these materials, the effective surfaces are unimportant and the notch strength of the material is determined solely by the maximum stress at the notch tip. This results in notch sensitivity. On the other hand, for the present cements, the Weibull modulus is very low compared to values for other engineering materials. Materials with lower Weibull moduli tend to be notch insensitive due to the competing effects of notch area and notch stress concentration. Note, however, that materials with even lower Weibull moduli may once again exhibit notch sensitivity that results from an increased sensitivity to notch surface area.

These findings are important from a clinical perspective as the size scale of notches examined in this work is representative of that which might be found at orthopedic repair sites employing self-setting bone cements. Understanding the response of brittle HA cements to the stress concentrating effects of such notches is clearly relevant for the reliability of fracture fixation and repair. In addition, the increased use of HA cements for more complicated repair sites requires a better understanding of their response to stress concentrators. The notch insensitivity of the two HA cements examined leads to the assertion that their use can augment orthopedic repair at sites where there are large or small inclusions without compromising their mechanical reliability. However, notwithstanding the insensitivity to the radius of the notch, it should be noted that the resulting strength of a cement repair site will always be reduced in the presence of a reduced section.

5. Conclusions

The tensile notch strength of two self-setting HA cements was examined for notch radii that ranged from 0.15 to 6 mm. The different notch radii had surprisingly little effect on the notch strength values. A weakest link fracture statistics model using Weibull statistics and modified to account for the presence of the notch was employed to rationalize the observed notch insensitivity of the two HA cements. The competing effects of notch tip stress fields and notch tip surface area were used to explain this phenomenon. These results have important implications for the reliable application of self-setting cements in load bearing orthopedic applications.

Acknowledgments

This work was supported by the Director, Office of Energy Research, Office of Basic Energy Sciences, Materials Science Division of the U.S. Department of Energy under Contract No. DE-FG03-95ER45543. Materials were provided by the Stryker Howmedica Osteonics and Norian Corporations. The authors thank Mr. Joseph Zitelli and Dr. George Faithful from Stryker Howmedica Osteonics for helpful discussions, Ms. Victoria Jew at Stanford University for technical assistance, and Dr. Theo Fett at the Forschungszentrum Karlsruhe, Germany, for assistance with the statistical analysis.

References

1. P. M. BILLS and E. J. WHEELER, *J. Ed. Mod. Mater. Sci. Eng.* **4** (1982) 391.
2. I. C. ISON, M. T. FULMER, B. M. BARR and B. R. CONSTANZ, in ''Hydroxyapatite and Related Materials'', edited by P. W. Brown (CRC Press, New York, 1994) p. 215.
3. W. E. BROWN and L. C. CHOW, in ''Cements Research Progress 1986'', edited by P. W. Brown (American Ceramics Society, Westerville, OH, 1987) p. 351.
4. B. R. CONSTANZ, I. C. ISON, M. T. FULMER, R. D. POSER, S. T. SMITH, M. VANWAGONER, J. ROSS, S. A. GOLDSTEIN, J. B. JUPITER and D. I. ROSENTHAL, *Science* **267** (1995) 1796.
5. L. L. HENCH, *J. Am. Ceram. Soc.* **74** (1991) 1487.
6. E. F. MORGAN, D. N. YETKINLER, B. R. CONSTANZ and R. H. DAUSKARDT, *J. Mater. Sci. Mater. Med.* **8** (1997) 559.
7. R. S. LAKES, S. NAKAMURA, J. C. BEHIRI and W. BONFIELD, *J. Biomech.* **23** (1989) 967.
8. V. C. JEW, J. P. MORGAN and R. H. DAUSKARDT, in ''Biomaterials for Drug Delivery and Tissue Engineering Procedures of the Fall MRS Conference Volume 662, Boston, Fall 2000'', edited by S. Mallapragada, M. Tracy, B. Narasimhan,

E. Mathiowitz and R. Korsmeyer (Materials Research Society, Warrendale, PA, 2000).
9. V. C. JEW, A. DURFEE, C. ANGLE and R. H. DAUSKARDT, in Transactions of the 46th Annual Meeting of the Orthopedic Research Society, Orlando, 2000.
10. V. C. JEW and R. H. DAUSKARDT, *J. Mater. Sci. Mater. Med.* 2002 (to be submitted).
11. L. J. GIBSON and M. F. ASHBY, in ''Cellular Solids: Structure and Properties'' (Pergammon Press, New York, 1998) p. 316.
12. T. L. ANDERSON, in ''Fracture Mechanics: Fundamentals and Applications'' (CRC Press, New York, 1995) p. 34.
13. W. BROWN and J. SRAWLEY, in ''ASTM Publication 410'' (American Society for Testing and Materials, Philadelphia, 1966).
14. J. R. MATTHEWS, F. A. MCCLINTOCK and W. J. SHACK, *J. Am. Ceram. Soc.* **59** (1976) 304.
15. A. BRUCKNER-FOIT, A. HEGER and D. MUNZ, *J. Europ. Ceram. Soc.* **16** (1996) 1027.
16. D. HERTEL, T. FETT and D. MUNZ, *ibid.* **18** (1998) 329.
17. T. FETT, D. HERTEL and D. MUNZ, *J. Mater. Sci. Lett.* **18** (1999) 289.
18. B. LAWN, in ''Fracture of Brittle Solids'' (Cambridge University Press, Cambridge, 1993) p. 31.
19. T. FETT, private communication, 2001.

Received 1 March 2002
and accepted 4 February 2003